A Quantitative Analysis of the Endocytic Pathway in Baby Hamster Kidney Cells

Gareth Griffiths,* Ruth Back,* and Mark Marsh‡

*European Molecular Biology Laboratory, D6900 Heidelberg, Federal Republic of Germany; and
‡Chester Beatty Laboratories, Institute of Cancer Research, London SW3 6JB, England

Abstract. A morphological analysis of the compartments of the endocytic pathway in baby hamster kidney (BHK) cells has been made using the fluid-phase marker horseradish peroxidase (HRP). The endocytic structures labeled after increasing times of endocytosis have been identified and their volume and surface densities measured. In the first 2 min of HRP uptake the volume density of the labeled structures increased rapidly and thereafter remained constant for the next 13–18 min. This plateau represents the volume density of endosome organelles and accounts for 0.65% of the cytoplasmic volume (or 6.8 μm^3 per cell). The labeled structures consist of tubular-cisternal elements which are frequently observed in continuity with 300–400 nm vesicles. After 15–20 min of internalization the volume density of HRP-labeled structures again increased rapidly and reached a second plateau between 30 and 60 min of labeling. This second increase corresponded to detectable levels of HRP reaching later, acid phosphatase (AcPase)-reactive compartments. These structures, comprising the prelysosomes and lysosomes, were mostly vesicular and collectively accounted for 3.5% of the cytoplasmic volume (or 37 μm^3 per cell). The absolute peripheral surface areas of the two classes of organelles (endosomes and prelysosomes/lysosomes) were estimated to be 430 and 370 μm^2 per cell, respectively.

The volume of fluid internalized in the first 2 min of uptake was five- to sevenfold less than the volume of the compartment labeled in this time. To account for these results we propose that, after uptake from the cell surface, HRP is delivered to, and diluted in, endosomes that are preexisting organelles initially devoid of the marker. With increasing times of endocytosis the concentration of HRP in the early endosomes increases, as more of the marker enters this compartment. An elevation in HRP concentration in endosomes during the early time points was shown directly using anti-HRP antibodies and colloidal gold on cryosections.

The stereological values given in the present study, in combination with earlier studies, provide a minimum estimate for both the total surface area of membranes and the rate of membrane synthesis in a BHK cell.

ENDOCYTOSIS is a property of eukaryotic cells whereby components of the extracellular medium are taken up in membrane-bound vesicles. Previous studies have identified a constitutive form of endocytosis in which components of the medium are internalized either nonadsorptively (fluid-phase endocytosis) or in association with specific receptors (receptor-mediated endocytosis) (Besterman et al., 1981; Helenius et al., 1983; Goldstein et al., 1985; Mellman et al., 1986). In baby hamster kidney (BHK) cells the constitutive endocytic activity is mediated predominantly by clathrin coated vesicles (Marsh and Helenius, 1980; Pearse and Bretscher, 1981) which form at the cell surface and subsequently fuse with and deliver their membrane and contents to endosomes. Within endosomes the internalized membrane components, ligands, and fluid content are sorted for subsequent redistribution to specific destinations in the cell (Simons and Fuller, 1985; Mellman et al., 1986).

In 1976 Steinman, Brodie, and Cohn published an important paper that provided the first quantitative estimates of the surface areas and volumes of the endocytic organelles in macrophages and L cells. The organelles were identified, and subsequently measured, using horseradish peroxidase (HRP)[1] which was taken into the cells by endocytosis. Since that publication, many aspects of the structure, function, and composition of endocytic organelles have been studied in considerable detail. It is now clear that the endocytic pathway can be subdivided into two major compartments, namely the endosomes, the organelles to which ligands and fluid are delivered after uptake from the cell surface, and the lysosomes,

1. *Abbreviations used in this paper*: AcPase, acid phosphatase; CB, cacodylate buffer; DAB, diaminobenzidine; HRP, horseradish peroxidase; LY, Lucifer Yellow; MPR, cation-independent mannose 6-phosphate receptor; NRK, normal rat kidney cells; TGN, *trans*-Golgi network.

the acid hydrolase-rich organelles in which ligands and fluid phase components are degraded. The endosome compartment can be further divided and appears to contain at least two functionally distinct subcompartments (Wall and Hubbard, 1985; Mueller and Hubbard, 1986; Murphy, 1985; Gruenberg and Howell, 1986, 1987; Gruenberg et al., 1989; Kielian et al., 1986; Schmid et al., 1988). The first, the early endosomes, receives all components internalized from the cell surface, and is the first site for sorting and recycling back to the plasma membrane. These organelles are morphologically complex and appear to reside in the peripheral cytoplasm (Wall et al., 1980; Helenius et al., 1983; Geuze et al., 1983; Hopkins and Trowbridge, 1983; Bergeron et al., 1985; Marsh et al., 1986; Gruenberg and Howell, 1987). The second compartment comprises the late endosomes. According to Mellman et al. (1986) these late organelles function both to receive material from the early endosomes and to deliver their contents into the lysosomes. Our recent data indicates that the late endosomes, defined in this way, encompass two distinct sets of structures. The first are spherical acid phosphatase (AcPase)-negative vesicular structures (referred to in this paper as endosome vesicles) that appear to require intact microtubules for further transport towards the lysosomes. (Gruenberg et al., 1989). The second is a more distal prelysosomal compartment that is highly enriched in the cation-independent mannose 6-phosphate receptor (MPR) and the lysosomal membrane glycoprotein Lgp 120, and is AcPase-positive (Griffiths et al., 1988; Griffiths, G., R. Matteoni, R. Back, and B. Hoflack, manuscript in preparation). The terminal lysosome compartment, where the bulk of acid hydrolase activity is localized, is also Lgp positive but essentially devoid of MPR. Although the structural and functional differences between these endocytic compartments are becoming more clear, their relationship to each other is less obvious. In particular, it remains open whether these organelles are preexisting entities in the cell or whether they arise de novo from the fusion of endocytic coated vesicles (Helenius et al., 1983).

In this paper we have made a morphometric study of the endocytic pathway in BHK cells. These cells have been used extensively in previous biochemical and morphological studies of endocytosis (Marsh and Helenius, 1980; Marsh et al., 1983, 1986, 1987) and for stereological studies of the compartments of the biosynthetic pathway (Griffiths et al., 1984*a*, 1989). We have compared the endocytic uptake of three markers (HRP, sucrose, and Lucifer Yellow) and have found that, in contrast to the situation in macrophages (see Swanson et al., 1985), HRP does not affect the rate of endocytosis in these cells and behaves as a true, nonadsorptive fluid-phase marker. By using both the conventional cytochemical reaction in plastic sections and immunocytochemistry on cryosections, we have used HRP to identify endocytic organelles. In addition, the cytochemical reaction for AcPase has been used to identify the lysosomal and prelysosomal compartments. These markers enabled us to perform a stereological analysis of the surface areas and volumes of endocytic organelles and the dimensions obtained have been compared with direct measurements of fluid-phase endocytosis. Together with measurements made previously, these data provide an estimate of the total area of membrane in a BHK cell and enable us to predict the minimum rates of membrane synthesis in a BHK cell.

Materials and Methods

Cells

Baby hamster kidney (BHK-21) cells were maintained in Glasgow's minimal essential medium (G-MEM) containing 5% FCS and 10% tryptose phosphate broth. For biochemical and morphological experiments, the cells were grown on 35-mm-diam tissue culture dishes for 2 d. In our earlier studies the mean cell volume was estimated using cultures that had just reached confluency (Griffiths et al., 1984*a*). Similar cultures were used here at a density of 3.2×10^5 cells per cm^3.

Biochemical Measurement of Fluid-phase Endocytosis

Fluid-phase endocytosis was measured essentially as described (Marsh and Helenius, 1980). Briefly, 35-mm dishes of cells in duplicate were washed once with G-MEM and then incubated at 37°C, with 0.5 ml prewarmed medium containing either 4 μCi ^{3}H-sucrose (6 Ci/mmol; Amersham International, Amersham, United Kingdom), 10 mg/ml HRP (Type 2; Sigma Chemical Co., St. Louis, MO) or 2 mg/ml Lucifer Yellow (LY) (Molecular Probes Inc., Eugene OR). At specified times the dishes were placed on ice and washed 10 times with ice-cold $Ca^{++}Mg^{++}$-free PBS. For reflux experiments the labeling medium was removed and the cells were washed 10 times in G-MEM and recultured in G-MEM at 37°C before washing with cold PBS. Subsequently the cells were scraped, transferred to centrifuge tubes, and washed three times with cold PBS by resuspending the cell pellet and centrifuging for 5 min at 1,500 rpm. The final cell pellet was resuspended in 0.5 ml PBS containing 0.1% Triton X-100 (Pierce Chemical Co., Rockford, IL) and 0.2% BSA. Total cell protein was determined using bicinchoninic acid (Pierce Chemical Co.) as described (Smith et al., 1985). ^{3}H-sucrose activity was assayed by counting aliquots of the resuspended cell pellets in a scintillation counter (model LS 7500; Beckman Instruments, Inc., Palo Alto, CA). HRP was determined using σ-dianisidine (Marsh et al., 1987) and LY was measured using a fluorescence spectrophotometer (model MPF-3L; Perkin Elmer Corp., Norwalk, CT) as described (Swanson et al., 1985).

Electron Microscopy: Epon Sections

The cells were washed once in fresh G-MEM and incubated at 37°C in prewarmed G-MEM containing 10 mg/ml HRP. Endocytosis was stopped at the required time by removing the medium, placing the dishes on ice, and washing twice (1-2 min each) with ice-cold PBS. The cells were then fixed with cold 1% glutaraldehyde in 200 mM cacodylate buffer (CB) pH 7.2, which was then allowed to warm to room temperature for 30 min. To visualize HRP, the fixed cells were rinsed with CB and incubated in CB containing 0.1% diaminobenzidine (DAB) for 1 min. The HRP-DAB reaction was initiated by adding H_2O_2, to a final concentration of 0.01%. After 2 min in the dark, the DAB solution was removed, the cells were washed in CB, postfixed for 60 min with 1% OsO_4, containing 1.5% potassium ferricyanide, and block stained for 1 h with 0.5% magnesium uranyl acetate in water.

AcPase was visualized by the lead capture method using β-glycerophosphate as substrate (Griffiths et al., 1983). For cells labeled with HRP the method was adapted as follows: the cells were fixed, and washed in several changes of CB followed by acetate buffer (pH 5.0). The preparations were then incubated in the β-glycerophosphate-lead nitrate medium containing 10% (vol/vol) dimethylsulfoxide for 75 min at 37°C. Subsequently, the samples were rinsed briefly in acetate buffer, returned to CB, treated with DAB, and then with osmium and uranyl acetate as above.

After these steps the preparations were rinsed with distilled water, dehydrated in ethanol and propylene oxide, and the cell monolayer removed during the latter step as described (Griffiths et al., 1984*a*). The cells were centrifuged to form a hard pellet (5 min at 13,000 *g*) and embedded in Epon.

Bovine serum albumin was conjugated to 5 nm gold particles at a concentration of 1 mg/ml. This was added to the culture medium at an OD_{520} value of 5.

Freeze Substitution

BHK cells that had internalized BSA-gold for 10 min at 37°C were placed on ice, removed from the monolayer with proteinase K, and centrifuged to form a pellet. Small pieces (<0.5 mm^3) of these pellets were rapidly frozen by plunging into liquid ethane cooled by liquid nitrogen (McDowall et al., 1989). The fragments of pellet were then transferred first into liquid nitro-

gen and then into a 5% solution of osmium tetroxide in acetone on dry ice (−70°C). The fragments were left in this solution overnight at −70°, then 2 h at −20°C, followed by 2 h at 4°C. After warming up briefly to room temperature the fragments were embedded in Epon.

Cryomicrotomy and Immunocytochemistry

Cryosections were prepared and labeled with antibodies and protein A-gold as described (Griffiths et al., 1984*b*). The cells, which had internalized 10 mg/ml HRP for 2, 5, or 10 min, were removed from the monolayer using 50 μg/ml proteinase K on ice (Green et al., 1981) and fixed with 1% glutaraldehyde in 200 mM Hepes buffer, pH 7.4. The anti-HRP antiserum was a kind gift of Drs. S. Avrameas and L. Teyrnick. Control incubations involved the use of antibodies to Semliki Forest virus and vesicular stomatitis virus (VSV).

For the quantitation of the anti-HRP labeling, 30 micrographs (primary magnification 17,000) of the cell cytoplasm were taken from random cryosections of appropriate thickness and preservation. By analogy to our earlier studies where the average section thickness was estimated to be 80–100 nm (Griffiths et al., 1984*b*), we assume our sections to be in this thickness range. After enlarging the negatives (×4.1) and using grid type A100 (Weibel, 1979), the number of points and the number of gold particles over labeled endosome structures were counted.

In a few experiments cells that had internalized BSA-gold (see above) for 5 or 10 min at 37°C were also prepared for cryosectioning.

Stereological Analysis

To determine the surface area and volumes of the various compartments in absolute units, an estimate of the mean cell volume of the BHK cell was required. In an earlier study (Griffiths et al., 1984*a*) we estimated this parameter to be 3,900 μm^3. It has since become evident that this value was overestimated by a factor of 2.4 (see Griffiths et al., 1989). We have recently used two different stereological methods to obtain a more accurate estimate of the mean cell volume (described in Griffiths et al., 1989). In addition Davoust et al. (1987) estimated the BHK cell volume by a biochemical method. The results using these methods were found to be in reasonable agreement and gave an average value of 1,400 ± 210 μm^3 for the BHK cell volume. We have used this estimate in the present study.

For each time point three Epon blocks were sectioned at random, and random micrographs were taken as described (Griffiths et al., 1984*a*). The micrographs were enlarged 4.1 times (linear) on a projector system designed at European Molecular Biological Laboratory. An acetate transparent sheet with an appropriate grid system was placed over the screen, and estimates of the surface and volume densities were made by point and intersection counting (Weibel, 1979). In this study a number of different single- and double-lattice grids type A100 or D64 (Weibel, 1979) were used with the required distance between the lines of the lattice value.

The analysis was done at three different levels, each at a different magnification.

Level 1. Primary magnification 2,800. By relating the number of points over the nucleus to those over the cytoplasm the volume density (volume fraction) of the cytoplasm (*cy*) per cell (*ce*) was estimated, that is Vv (*cy,ce*).

Level 2. Primary magnification 17,000. A double-lattice grid (D64) was used (Weibel, 1979). By counting the number of the "large" points of the double-lattice grid over cytoplasm and the number of "small" points of the double-lattice grid over the structure of interest the volume densities of the following organelles were estimated: tubules of early endosomes, Vv(*en-t,cy*); vesicles of early endosomes, Vv(*en-v,cy*); prelysosomes and lysosomes, Vv(*l,cy*); mitochondria, Vv(*mit,cy*).

Level 3. Primary magnification 28,000. By relating the number of points of the lattice grid (A100) over the structure of interest with the number of intersections with its outer limiting membrane the surface densities, Sv (or surface to volume ratios) of the following parameters were estimated: tubules of early endosomes, Sv(*en-t,en-t*); vesicles of early endosomes, Sv(*en-v,en-v*); prelysosomes and lysosomes, Sv(*l,l*); outer mitochondrial membranes, Sv(*om,mit*); inner mitochondrial membranes, Sv(*im,mit*).

The volume density is estimated from the ratio of the total number of points over the structure (*x*) to the total number over the reference space (in most cases the cytoplasmic volume, *cy*).

$$Vv = \frac{\Sigma\, Px}{\Sigma\, Pcy}.$$

The surface density, Sv, is estimated as

$$Sv = \frac{\Sigma\, I}{\Sigma\, Pd},$$

where I is the number of intersections with the grid in both vertical and horizontal directions, *P* the number of points, and *d* the distance between points. When *d* is given in microns, Sv is obtained in units of microns^{-1}. Computation was done according to the method of Cruz-Orive (1982), as described previously (Griffiths et al., 1984*a*). In the tables the data are expressed as mean ± standard error of the mean.

Correction Factors

Section compression is unlikely to contribute a significant error to the stereological estimates (see Griffiths et al., 1984*b*) and was ignored. The Sv estimates were made at a final magnification of 115,000 in order to avoid "resolution effects" (Paumagärtner and Weibel, 1978). The vesicular and cisternal structures estimates here are all significantly larger than the average section thickness (~40 nm). However, the diameter of the endosome

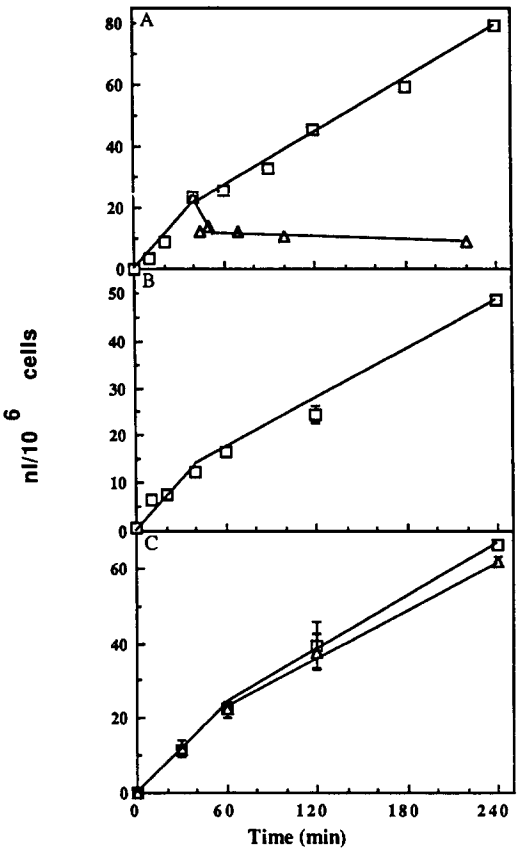

Figure 1. Fluid-phase endocytosis in BHK-21 cells. Confluent dishes of BHK-21 cells were incubated in medium containing ^{3}H-sucrose (*A*), HRP (*B*), or Lucifer Yellow (*C*) at 37°C. At the times indicated, the dishes were placed on ice, the cells washed thoroughly with 0°C PBS, and the cell-associated radioactivity and total protein determined as described in Materials and Methods. For each marker fluid-phase endocytosis was calculated from the initial specific activity of the marker in the medium and is expressed as nanoliters of fluid internalized per microgram cell protein and converted to nl/10^6 cells. A second series of dishes (△) in *A* were incubated with ^{3}H-sucrose for 40 min at 37°C, washed, and incubated in medium without ^{3}H-sucrose for between 5 min and 3 h at 37°C. Subsequently, the cells were placed on ice, washed, and the cell-associated radioactivity and protein determined. In *C* the plates were incubated in media containing Lucifer Yellow (□) or media containing Lucifer Yellow and HRP (△).

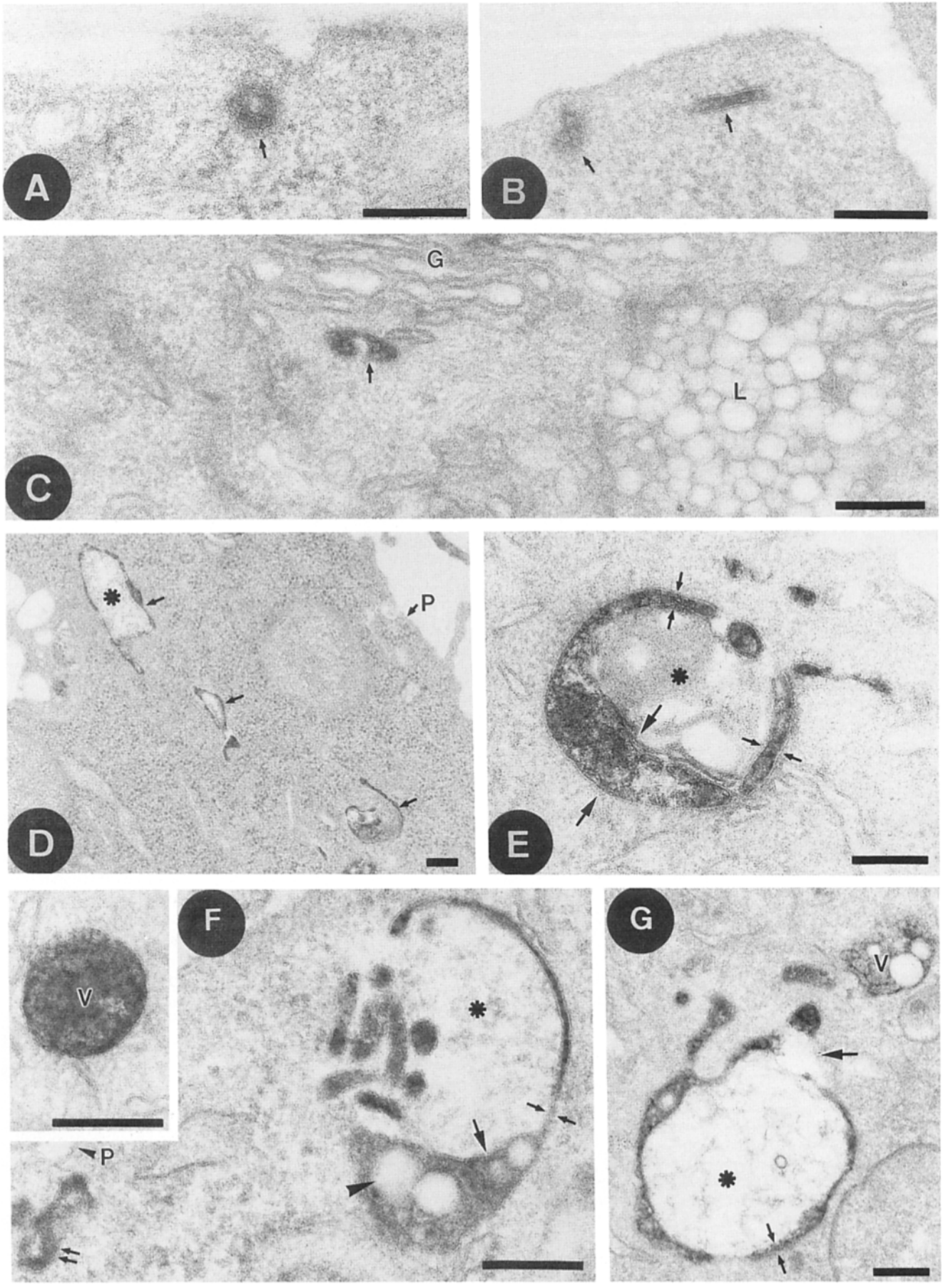
A
B
G
L
C
P
D
E
V
F
P
G
V

tubules is often less than the section thickness. Therefore a correction factor has been derived for the Holmes, or overprojection, effect (Weibel, 1979). For this correction we have assumed that all endosomal structures <80 nm diam are tubular (in fact this is not the case; serial sections revealed that some, though not all, of the tubular profiles <50 nm diam were sections through endosomal cisternal elements [see below]). The method involves estimating the section thickness, the mean diameter (d), and the mean length (D) of profiles of the tubules in random sections. From these parameters the correction factor can be determined from the graphs found in Weibel (1979). Stereological principles are ideally suited to "infinitely thin sections." The more deviation from this ideal (i.e., as section thickness increases), the greater the error. Correction factors were therefore derived for three different thicknesses of sections, estimated by the fold procedure (Small, 1968), in order to get an approximate idea as to how much section thickness might influence the overprojection effect. We emphasize that, since we do not know the proportion of the <80-nm profiles that are tubular, these correction factors are only approximate and can only give an impression of the magnitude of error that is possible.

*Table I. Correction Factors for Vv of Endosome Tubules**

Section thickness‡	Mean diameter (d)	Mean profile length (D)	Correction factor, K
nm	*nm*	*nm*	
21.4	36.2 ± 1.3	238.8 ± 20	0.75
39.6	40.2 ± 2.3	236.5 ± 20	0.62
65.5	46.8 ± 1.9	294.3 ± 28	0.55

* Assuming that all the tubulo-cisternal endosome structures were made up of real tubules only. For a detailed description of how these correction factors are estimated, and the assumptions therein, see Weibel, 1979.
‡ Determined using the fold procedure of Small (1968).

Results

Fluid-phase Endocytosis

HRP has been used extensively in morphological and biochemical analyses of endocytosis (see, for example, Steinman et al., 1976; Marsh and Helenius, 1980; Marsh et al., 1986; Swanson et al., 1985; Sullivan et al., 1987; de Chastellier et al., 1987). However, Swanson et al. (1985) found that HRP can increase the endocytic activity in thioglycollate-stimulated murine peritoneal macrophages. In addition, they confirmed that HRP does not recycle in macrophages (Steinman et al., 1976) and questioned the use of this reagent as a nonadsorptive marker of constitutive endocytosis in macrophages. To ensure that HRP could be used as a fluid-phase marker in BHK-21 cells, we examined the uptake of three chemically different fluid-phase markers. Confluent 35-mm dishes of cells were incubated for up to 4 h in 37°C medium containing ^{3}H-sucrose, HRP, or LY. Subsequently the cells were washed, the cell-associated activity determined, and the fluid volume internalized was estimated from the specific activity of the medium. Uptake was proportional to the concentration of the label in the medium (not shown) for each marker and displayed biphasic kinetics (Fig. 1). Some variation was observed in the accumulation of the different markers. During an initial phase of uptake, between 0 and 45 min, the cells internalized ^{3}H-sucrose-containing medium at a rate of 34 nl/10^6 cells/h (or 0.57 μm^3/cell per minute; Fig. 1 *A*) and medium containing HRP (Fig. 1 *B*) or LY (Fig. 1 *C*) at a rate of 25 nl/10^6 cells/h (or 0.42 μm^3/cell per minute). After 40–60 min the rate of uptake declined to 27 nl/10^6 cells/h for ^{3}H-sucrose-containing medium (12 nl/10^6 cells/h for HRP and LY) and remained constant for a further 3 h. The differences in the uptake of three markers is not understood, but some variation can be expected as a consequence of the different ways in which the cells will handle three chemically different markers. The variation in the initial rates of uptake is <30% and subsequent calculations have been made using the values as upper and lower estimates of fluid phase uptake. The estimate for the uptake of ^{3}H-sucrose is similar to that previously published for BHK cells (Marsh and Helenius, 1980).

The biphasic accumulation of cell-associated label arises as a result of recycling of a portion of the internalized marker to the medium. The initial phase of uptake provides an estimate for the volume of fluid-phase uptake alone. The later accumulation of marker, which occurs after 60 min of endocytosis, reflects the steady state situation when endocytosis and recycling have reached equilibrium. At this stage the accumulation of marker reflects the transfer of internalized fluid to later stages of the endocytic pathway from which recycling is either nonexistent or of relatively small magnitude (Besterman et al., 1981; Swanson et al., 1985). To confirm that internalized label is recycled, BHK cells were labeled for 40 min, washed, and recultured in marker-free medium at 37°C. An experiment with ^{3}H-sucrose is shown in Fig. 1 *A*. Within 10 min the cell-associated radioactivity declined to ~50% of that at the beginning of the chase and over the next 3 h decreased further by 10–15%. Similar recycling was observed with HRP (not shown).

The relatively similar rates of fluid-phase endocytosis measured with the three different markers suggested that uptake was not influenced by the markers themselves. Since Swanson et al. (1985) had shown that HRP can stimulate fluid-phase uptake in macrophages, we measured LY uptake both in the presence and absence of HRP. The results (Fig. 1 *C*) show that the presence of 10 mg/ml HRP did not significantly affect the uptake or accumulation of LY in BHK cells.

Figure 2. *A–C* show Epon sections of BHK cells that had internalized HRP for 30 s. In *A* a clathrin coated vesicle is seen (*arrow*). In *B* small labeled profiles are evident near the plasma membrane (the profile on the left may be a coated vesicle). In *C* one of these labeled profiles is seen in close proximity to a Golgi stack and a larger unlabeled structure (*L*) which is either a prelysosome or lysosome. In *D* (5-min HRP), *E*, *F*, and *G* (10-min HRP) typical endosome structures are apparent. In *D*, at low magnification, three endosome profiles can be seen (*arrows*). In *E*, *F*, and *G*, higher magnification, the main features are tubulo-cisternal projections (*small arrows*) in continuity with larger vesicular profiles (*large arrows*). The asterisks in *D–G* indicate the electron-transparent area that is partially enclosed by the endosome structure; in *E* some ill-defined structural feature is evident in this area. The arrowhead in *F* indicates vesicular inclusions within the endosome vesicle. An endosome profile is also indicated next to the plasma membrane (*P*) by the small double arrows. The inset in *F* shows an apparent free endosome vesicle (*V*). In *G* the large arrow shows an area where the tubulo-cisternal part of the endosome is clearly artifactually fractured or extracted, giving a clear example of the lability of endosomes. Bars, 200 nm.

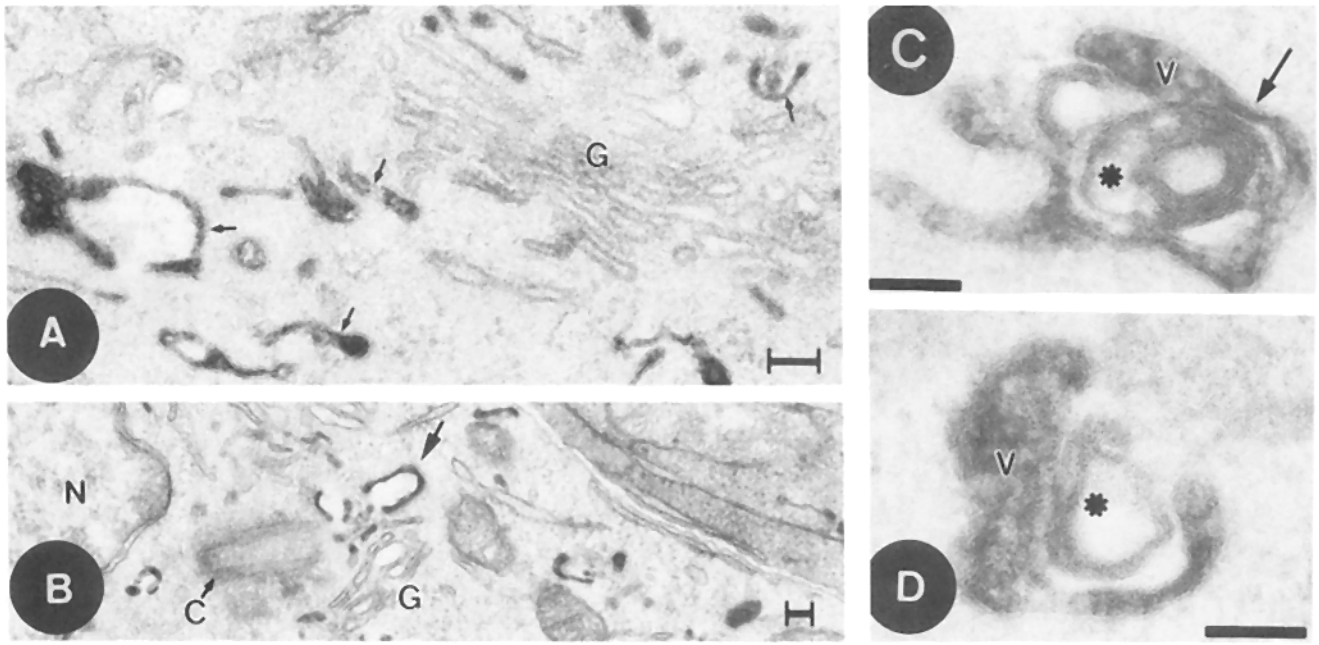

Figure 3. Structure of endosomes in Epon sections. *A* and *B* show HRP-labeled profiles (*arrows*) in close vicinity to the Golgi complex (*G*) and the centriole (*C*) (*A*, 20-min HRP; *B*, 30-min HRP). *N*, nucleus. *C* and *D* show myelin-like membrane arrays in the space (*asterisk*) enclosed by the endosome tubulo-cisternal structures in cells labeled for 2 min with HRP. For reasons explained in the text we believe these myelin-like structures are artifacts. Bars, 100 nm.

Morphology of HRP-labeled Organelles

The biochemical estimates of endocytosis demonstrate that HRP is treated as a fluid-phase marker by BHK cells and can, therefore, be used as a marker to identify organelles involved in fluid-phase endocytosis. BHK cells were incubated with HRP at 37°C for times between 30 s and 2 h, washed, fixed, and treated with DAB. The labeled organelles were then identified by the electron dense HRP–DAB reaction product. En bloc staining with magnesium uranyl acetate improved the fine structure preservation of the organelles and enabled a number of features to be seen that had not been apparent in our previous study.

From as early as 30 s after the onset of labeling, HRP-containing coated vesicles (Fig. 2 *A*) and tubular elements (Fig. 2 *B*) could be seen in the cell periphery and occasionally deeper in the cytoplasm (Fig. 2 *C*; see below). In cells labeled for 2 min or longer, other endosomal structures, larger vesicles and numerous tubular profiles, became apparent (Fig. 2, *D–G*). Serial sections indicated that a number, though not all, of the tubular profiles were sections through cisternal-like structures, that is, membranes aligned in parallel that extend through a number of sections in a series. The mean membrane-to-membrane spacing for these tubular/cisternal structures was 36.2 ± 1 nm in a 21-nm section and 46.8 ± 2 nm in a 65-nm section (Table I). Many of the structures, previously considered as vacuoles, appeared as bowl-shaped cisternae (Figs. 2, *D–G*, and 3 *A*) and often enclosed a myelin-like membrane structure which appeared, in some micrographs, to be continuous with the membrane of the cisternae (Figs. 2 *E*, and 3, *C*, and *D*). In a number of cases this structure seemed to be extracted during specimen preparation and appeared as an electron-transparent zone (*asterisks* in Fig. 2, *F* and *G*). The dimensions of the myelin-like membrane structures, which we believe to be preparation artifacts (see Discussion), are not included in the estimates of endosome surface area and volume.

Parts of the cisternal structures were enlarged and contained tubulo-vesicular membrane profiles in their lumen (Fig. 2, *E* and *F*). Spherical vesicles (Fig. 2 *F*, *inset*), with similar internal contents, were seen in serial sections both with, and without, obvious attachment to other endosomal components. The mean diameter of the vesicular structures that labeled up to 15 min was found to be 162 ± 12 nm. These measurements exclude those vesicles with diameters of 80 nm or less.

Even after 30 s of HRP internalization HRP-labeled profiles could be seen close to elements of the Golgi complex (Fig. 2 *C*) and the centriole. At times later than 2 min the frequency of these structures increased (Fig. 3, *A* and *B*). It should be noted that in many cultured cells the Golgi complex is often found close to the plasma membrane. Thus in the absence of markers, endocytic structures such as that shown in Fig. 2 *C* would be morphologically indistinguish-

Figure 4. Epon sections of HRP-labeled prelysosomes and lysosomes. In *A*, after 25-min internalization, the appearance of larger labeled vesicular structures is evident (*arrows*) adjacent to similar structures that are unlabeled (*asterisks*). *B* shows an example of a lysosome or prelysosome structure labeled for 90 min at 37°C that contains a large electron-transparent core (*asterisk*). The arrows indicate myelin-like membranes. *C* and *D* show examples of tubular lysosomes after 2 h of labeling at 37°C. Bars, 200 nm.

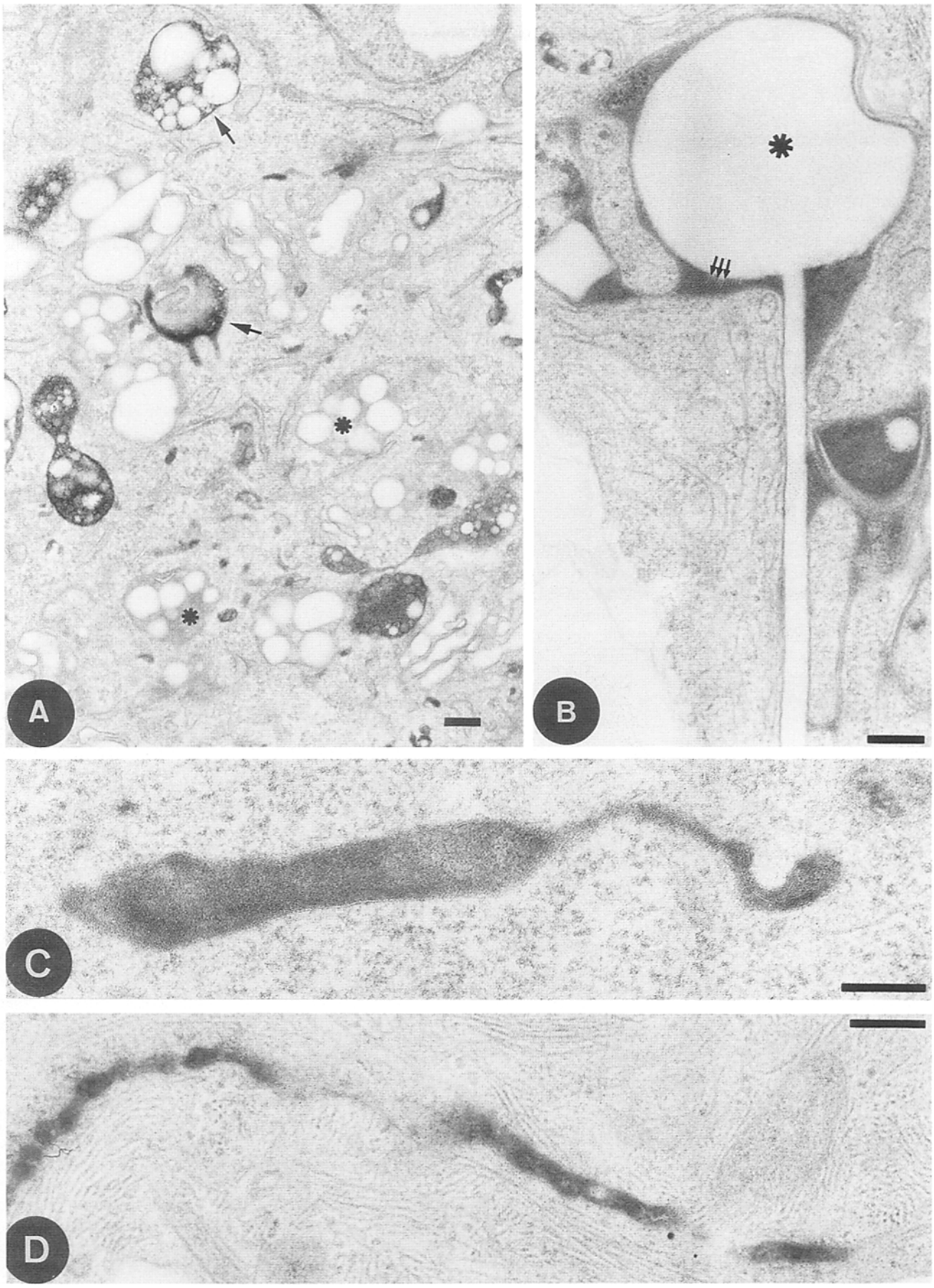
A
B
C
D

able from components of the *trans*-Golgi network (TGN [Griffiths and Simons, 1986]).

After 20 min of HRP internalization many different kinds of labeled structures were seen (Figs. 3 and 4). These were large vesicles (up to 3 μm diam) with vesicular contents and with tubular extensions (Fig. 4). Many of these structures contained internal membranes (Fig. 4 *B*) and were reminiscent of the MPR-enriched prelysosomal structures seen in normal rat kidney (NRK) cells (Griffiths et al., 1988). In addition, long tubular (or cisternal) structures were occasionally observed (Fig. 4, *C* and *D*) which appeared similar to "tubular lysosomes" (Swanson et al., 1987). Finally, some of the larger vesicles and their tubular extensions contained large, often rod-shaped, electron-transparent structures (Fig. 4 *B*) reminiscent of the cholesterol crystals that accumulate in the lumen of AcPase-reactive vesicles in cells of animals kept on a high cholesterol diet (Shio et al., 1979).

From reasons given in the Discussion, as well as from the AcPase data described below, we assume that the structures that label after 20–30 min HRP internalization correspond to a combination of prelysosomes and lysosomes.

Morphology of the Early Endosomes after Freeze Substitution

The curved, bowl-shaped early endosome cisternae are very distinct and unexpected structures. To confirm that this organization was not due to our specimen preparation protocol we used two additional approaches to visualize the structures: if a structure is artifactually altered by one approach it would seem unlikely that it would be similarly affected by a different protocol. The first alternative was freeze substitution of cells that had internalized BSA-gold for periods up to 15 min at 37°C. The second was to cryosection aldehyde-fixed cells (see below).

For freeze substitution, cells were rapidly frozen and then treated overnight with osmium tetroxide in acetone at −70°C, followed by gradual warming to, and embedding in Epon at, room temperature. Although the cells are chemically fixed by the osmium, the procedure is quite different from the conventional aldehyde fixation followed by osmium at physiological temperatures. Since HRP cannot be used as an endocytic marker in freeze-substituted samples, an alternative label was required. For this purpose BSA-gold conjugates were used. Fig. 5 shows, using conventional Epon sections and DAB, that HRP and BSA-gold are internalized into the same endocytic vesicles. The structure of the early endosomes marked by BSA-gold in the freeze-substituted, Epon-embedded preparations of BHK cells (Fig. 6) was virtually identical to that seen with the DAB reaction product after conventional embedding.

Volume of the Endocytic Compartments

The volume density (volume fraction) of the endocytic organelles was determined as described in Materials and Methods. After 30 and 60 s of endocytosis, the volume density of the HRP-labeled structures was 0.07 and 0.10%, respectively (Fig. 7). The volume of the labeled structures then increased rapidly up to 2 min of labeling and corresponded to the appearance of HRP in larger tubulo-vesicular organelles. Between 2 and 15–20 min the volume of the labeled organelles remained approximately constant (Fig. 7).

Previous biochemical and cell fractionation experiments using BHK cells have shown that ligands internalized by receptor-mediated endocytosis, or HRP taken up by fluid-phase endocytosis, first enter a degradative compartment 15–20 min after uptake from the cell surface (Marsh et al., 1983; unpublished data). The data of Gruenberg et al. (1989) for BHK cells, and Schmid et al. (1988) for Chinese hamster ovary cells, indicate that by 15 min the HRP will have gained access to two functionally distinct endosome compartments. Since the volume density of the HRP-labeled structures was constant from 2 to 15 min after the addition of HRP, we assume that the mean of the estimates taken between these time points, 0.65%, is an indication of the volume density of two distinct endosome compartments. In agreement with the latter suggestion, we could distinguish two types of structures labeled within 15 min of HRP uptake. These were the tubules or cisternae, with profile diameters less than about 80 nm, and the vesicular structures with profile diameters exceeding 80 nm (see above). Using these criteria the volume density measurements indicated that 72% of the volume of the endosomes (0.47% of the cytoplasmic volume) was in tubulo-cisternal structures and 28% (0.18% of the cytoplasmic volume) was in the vesicular profiles (Table II). Assuming a cytoplasmic volume of 1,050 μm^3 (Griffiths et al., 1989) the absolute volume of the endosomes per BHK cell was calculated to be 6.8 μm^3 (Table III). Of this, endocytic coated vesicles probably represent <10% of the total endosome compartment. Assuming that endocytic coated vesicles have an internal diameter of 100 nm and an internal volume of $5 \times 10^{-4}/\mu m^3$, then the number of vesicles required to internalize 0.42–0.57 μm^3 fluid-phase each minute would be 850–1,130.

Between 20–30 min of HRP uptake the volume of the labeled compartment doubled while that of the tubular-cisternal structures increased by 60% (Fig. 7). As discussed above this increase in volume density corresponded to the delivery of HRP to late endocytic compartments. The increase in volume compared to the endosome organelles defined by the 15 min time point was equivalent to ~0.9% of the cytoplasmic volume. After the second increase, the total volume of the HRP-labeled structures remained relatively constant until the end of the labeling period at 2 h. Thus, the volume of the late endocytic compartments accessible to HRP after 2 h at 37°C was 9.4 μm^3/cell.

After incubation of cells with HRP for 2 h at 20°C, a condition that blocks endosome to lysosome transport (Marsh et al., 1983), the volume density of the labeled organelles was 0.81%, 20% larger than the volume of the endosome compartment measured after 15 min at 37°C (Table II). Colocalization of HRP and AcPase suggested that this increase is due to some HRP entering the AcPase-positive prelysosomal compartment at 20°C (not shown).

The diameters of the endosome tubules we measured approached, or were less than, the average section thickness. Consequently the volume measurements may be exaggerated due to the Holmes or overprojection effect. Weibel (1979) has outlined methods to arrive at correction factors for this phenomenon. For these corrections we must first assume that the whole of the tubular part of the endosome is made up completely of finger-like tubules rather than extensive cisternal sheets. As described above this assumption is not completely valid. However, we wanted to get an idea of the possible magnitude of any error. Table I lists the three parameters esti-

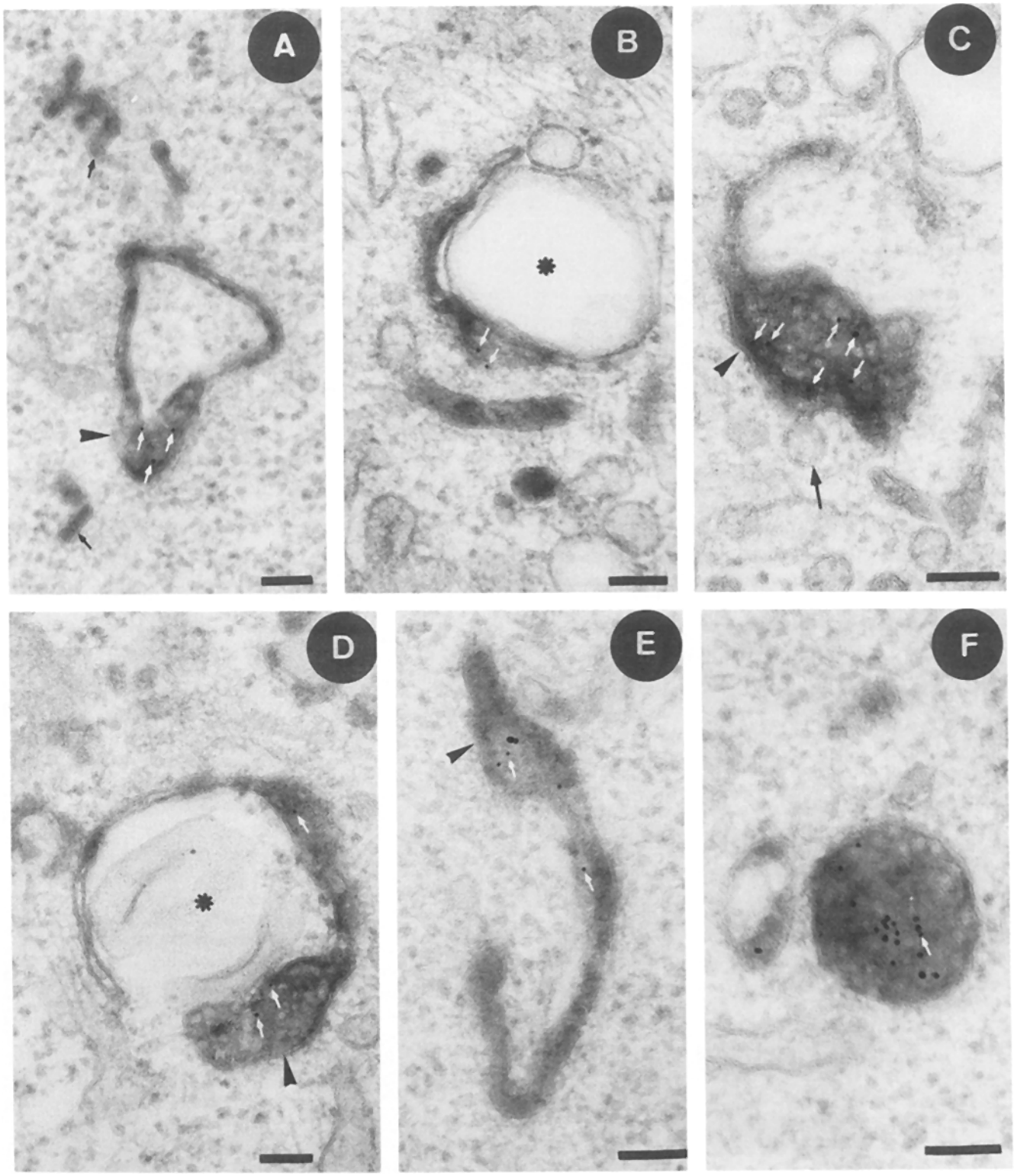

Figure 5. Epon sections of cells that had internalized 10 mg/ml HRP and BSA–gold for 10 min at 37°C. Most of the gold particles are indicated by white arrows. In *A* a section through a cup-shaped reticular part of the endosome is evident as is the widening in its lower part (*arrowhead*). Adjacent tubular profiles are also seen (*arrows*). *B* and *D* indicate the curved cisternal structures surrounding an amorphous area (*asterisks*) that are reminiscent of liquid droplets. The arrowheads in *C*, *D*, and *E* show the enlarged "vesicular" parts that are in continuity with the cisternal structures. A similar continuity is also evident in *C*, which also shows an apparently unlabeled vesicle (*large arrow*) in continuity with the labeled endosome. *E* shows an example of a more extended form of an endosome reticular structure. *F* indicates an endosome vesicle. Bars, 100 nm.

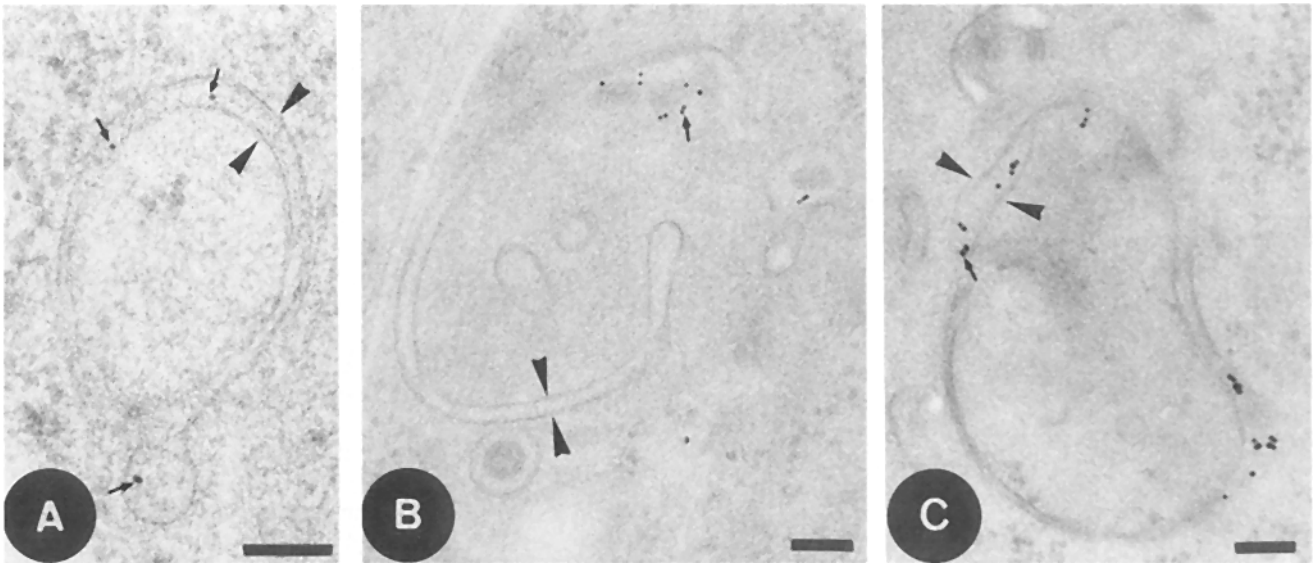

Figure 6. Epon sections of freeze-substituted BHK cells that had internalized BSA–gold (*arrows*) for 10 min at 37°C. Although the contrast of these sections is not ideal the cup-shaped endosome cisternal structures are clearly visualized: the arrowheads indicate the two closely opposed membranes. Bars, 100 nm.

mated on sections of three different thicknesses. In Table III we have added the corrected Vv values for the endosome tubular-cisternal parts in order to show what they would be if we assumed (arbitrarily) that the real (finger-like) tubules made up 50% of the volume of endosomes. These corrections would reduce our volume and surface estimates for the endosome by up to one-third.

Increase in HRP Concentrations in Endosomes: Structure of Endosomes in Cryosections

Our biochemical estimates indicated that BHK cells internalize 0.42–0.57 μm^3 of fluid per cell per minute. In 2 min a cell will internalize 0.84–1.13 μm^3, and in 15 min 6.2–8.5 μm^3. The volume of the HRP-labeled organelles, estimated morphometrically, increased rapidly to 6.8 μm^3 after 2 min and then remained constant for a further 13–18 min. With the given rate of internalization it should take 12–15 min to internalize 6.8 μm^3 of fluid. The simplest interpretation of these data is that incoming HRP is initially delivered from a relatively small pool of coated vesicles to larger, initially marker-free organelles. If this is true then the concentration of HRP in endosomes should increase from 2 to 15 min.

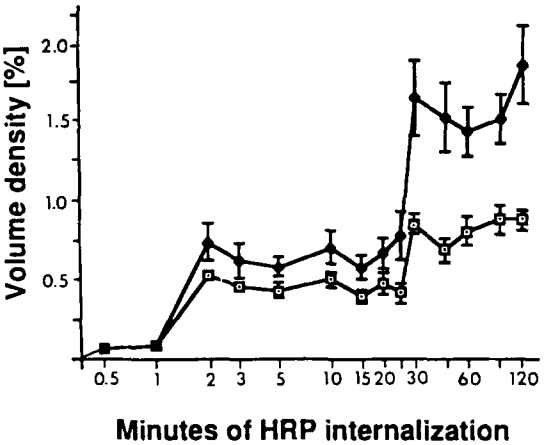

Figure 7. Stereological estimates of the volume density of HRP-labeled structures with time (semi-log scale). The ordinate (Vv) is volume density in percent with respect to the BHK cytoplasmic volume. The open squares show the values for the tubular-cisternal structures while the solid squares indicate those for the total of tubulo-cisternal as well as the vesicular structures (profiles >80 nm). For each point the error bars show the standard errors of the means for the micrographs that were pooled from two experiments.

To determine whether the marker concentrations in endosomes varied, BHK cells were labeled for 2, 5, or 10 min with HRP at 37°C, then washed, fixed, and processed for cryo-ultramicrotomy. Thin cryosections were thawed, and incubated with rabbit antibodies against HRP followed by protein A–gold. The HRP-containing structures observed (Figs. 8 and 9) were morphologically similar to those seen in plastic sections. In the cryosections several features of the endosomes were clearer than in Epon sections and the complex nature of the endosome tubulo-cisternal parts, in particular, was often more easily appreciated. Significantly, the gold particles, indicative of HRP, were localized predominantly to the periphery of the tubulo-cisternal structures. As

Table II. Volume Density of HRP-labeled Endocytic Organelles and AcPase-positive Structures

Condition	*n*	Vv‡
Endosome tubules, HRP 37°C*	100	0.47 ± 0.06
Endosome vesicles, HRP 37°C*	100	0.18 ± 0.02
Early endosome total, HRP 37°C*		0.65 ± 0.08
Early endosome total, HRP 20°C		0.81 ± 0.09
HRP 2 h − 37°C, 2-h chase at 37°C	20	3.8 ± 1.0
AcPase structures, 37°C§	27	3.5 ± 0.8

n, number of micrographs.
* These data are the average of the values between 2- and 15-min HRP internalization (see Fig. 2).
‡ Vv is volume density with respect to BHK cell cytoplasmic volume.
§ These are referred to as prelysosomes and lysosomes collectively in the text.

Table III. Estimation of the Sv and Absolute Volumes and Surface Areas per BHK Cell

Organelle	Absolute volume per cell*	Sv	Absolute surface per cell*
	μm^3	μm^{-1}	μm^2
Endosome vesicles‡	1.9 ± 0.4	19.5 ± 1.5	37 ± 8
Endosome tubulo-reticular parts	4.9 ± 1.2	80.1 ± 1.3	393 ± 97
(corrected)§	(3.0 ± 0.7)		(244 ± 60)
Endosome total	6.8 ± 1.6		430 ± 105
Lysosome and prelysosome	36.8 ± 11.2	10.1 ± 0.7	370 ± 113

* Assuming 1,050 μm^3 for the cytoplasmic volume (Griffiths et al., 1989).
‡ Vesicles here is defined as any labeled structure that has a diameter >80 nm.
§ Correction assuming the correction factor 0.62 from Table I. Note that since these correction factors have a number of assumptions inherent to them (see text) it is difficult to be confident of their validity.

with the DAB reaction (Fig. 2, *G* and *F*), the gold was often clearly seen between the two membranes of a cisternae (Fig. 8, *B* and *C*). In other cases, the particles were predominantly on the periphery of the structure (Figs. 8 *A* and 9 *A*), but an inner membrane was not clearly visualized. It was also evident was the fact that the vesicular and tubular membranes within the lumen of early endosome vesicles stood out more clearly in cryosections (Fig. 8, *D–F* and 9 *A*). Finally, images suggestive of coated domains were observed (Fig. 9 *B*). The nature of these coats is unclear but, from earlier studies (Geuze et al., 1983), we presume that at least some are composed of clathrin.

The density of gold particles over endosomes in cells incubated with HRP for 10 min was approximately three- to fivefold higher than the density of particles over the organelles in the 2-min labeled cells (Fig. 10). This increase in density was observed first in the tubulo-cisternal portions of the endosome compartment and subsequently in the endosome vesicles. Significantly, the density of label over the tubulo-cisternal parts of the endosome was higher than that over the vesicular parts, even in cases where the two structures appeared continuous. It is unclear whether this reflects a genuine variation in the HRP concentration within the two structures, or is simply due to variable labeling efficiencies arising, for example, from differences in the accessibility of antibodies to the antigen. However, the data are consistent with the notion that the HRP concentration in endosomes increases in the first few minutes after uptake and that the tubulo-cisternal structures are proximal to the vesicular ones.

An alternative way to visualize the endosome structures in cryosections was to look at the cells that had internalized BSA–gold (see above). Both the tubulo-cisternal parts of the endosomes, including the curved bowl-shaped cisternae and the endosome vesicles (Fig. 11) appeared very similar to the organelles observed in the other preparations (above).

Volume of the AcPase-reactive Structures

AcPase has been used extensively as a cytochemical marker for lysosomes (Novikoff and Novikoff, 1977). This marker is not, however, limited to lysosomes, but also appears in variable amounts in the TGN and the Golgi stacks (Novikoff and Novikoff, 1977; Hand and Oliver, 1984; Griffiths and Simons, 1986). Recently, we found that the MPR-enriched prelysosomal compartment in NRK cells is the first station on the endocytic pathway that reacts significantly for AcPase (Griffiths, G., R. Matteoni, R. Back, and B. Hoflack, manuscript submitted for publication). To determine whether the increase in the volume of the HRP-labeled compartment observed after 20 min of endocytosis corresponded to delivery of the marker to prelysosomes and lysosomes, we compared the volume of the HRP-reactive structures distal to the endosomes with the volume of the endocytic structures that react for AcPase.

We did not want to include the TGN or other parts of the Golgi complex in these estimates. Since the TGN contains primarily tubular-cisternal structures (Griffiths et al., 1989) and most of the late endocytic structures are large vesicular organelles (>100 nm) we counted only those AcPase-reactive structures with profile diameters >100 nm. The result (Table II) indicates that 3.5% of the cytoplasmic volume (37 μm^3 per cell) was occupied by these large vesicular structures. This value must obviously be considered an underestimate, as any tubular-cisternal parts of late endocytic structures are not included. Note, however, that the tubular-cisternal parts of late endocytic structures (between 20- and 120-min internalization) can only be expected to account for ~0.25% of the cytoplasmic volume (Fig. 7).

After 2-h incubation with HRP the total volume of labeled structures accounted for 1.5% of the cytoplasmic volume (Fig. 7). Since the endosomes account for 0.65%, it can be concluded that HRP-reactive distal structures that labeled after 2 h comprised only 0.85% of the cytoplasmic volume or ~25% of the AcPase-positive structures.

To determine whether longer incubations with HRP would fill the remaining organelles, or whether a significant proportion of lysosomes are not functionally connected to endosomes, we incubated cells with HRP for 2 h and then chased the label for a further 2 h in HRP-free medium. In this way, only the distal compartments should be visualized. After a 2-h pulse and a 2-h chase, the volume density of HRP-labeled structures was similar to that estimated for the total AcPase-reactive vesicles, suggesting that the whole population of AcPase-reactive vesicles were now accessible to the marker (Table II). The mean diameter of these HRP-reactive vesicles was 524 ± 30 nm.

Surface Area of Endosomes, Lysosomes, and Coated Pits

From the volume density of a membrane compartment the surface density (Sv) (or surface to volume ratio) can be estimated from high magnification micrographs by relating intersections of a lattice grid to the area (measured by "points") of the grid lying over the compartment of interest. The Sv for endosome tubules, vesicles, and for lysosomes are given in Table III. Note that these estimates only consider the outer, limiting membranes of the structures and the internal membranes were not scored. By multiplying the absolute volume of these compartments per cell by their surface densities the absolute surface areas per cell were estimated. The results indicate that the total surface area of endosomes per average BHK cell is 430 μm^2 and that of the prelysosomes and lysosomes 370 μm^2. By measuring the ratio of intersections of the lattice grid with coated pits relative to the total

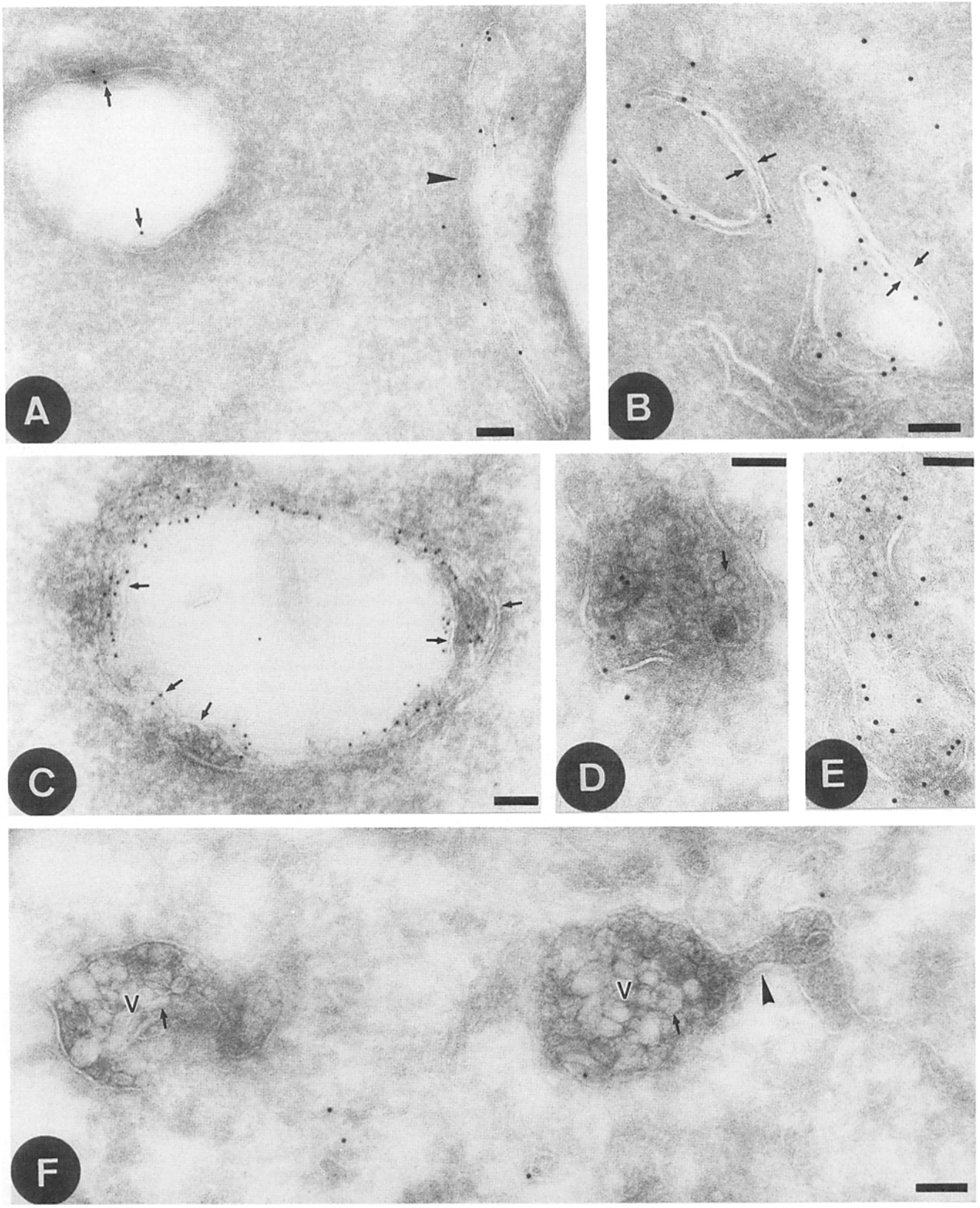

Figure 8. Cryosections of BHK cells that had internalized HRP for either 2 (*A*, *D*, and *F*) or 10 min (*B*, *C*, and *E*) that were labeled with anti-HRP followed by protein A–gold (*arrows* in *A*). In *A* a tubulo-cisternal part of the endosome appears as a vesicle although the HRP reaction is mostly confined to the "periphery" (*arrows*). It is likely that the periphery is made up of two closely opposed membranes that are enclosing a (cytosolic?) space (cf. Figs. 2, 5, and 6). In *B* and *C* the inner and outer membranes are more distinct (*arrows*). The arrowhead in *A* indicates a cisternal profile. In *D*, *E*, and *F* endosome vesicle structures are shown. Note the membranous contents (small arrows in *D* and *F*). The arrowhead in *F* indicates a continuity between the vesicular part of the endosome and a tubulo-cisternal part. Such images suggest that these vesicles may bud-off from the early endosome. Bars, 100 nm.

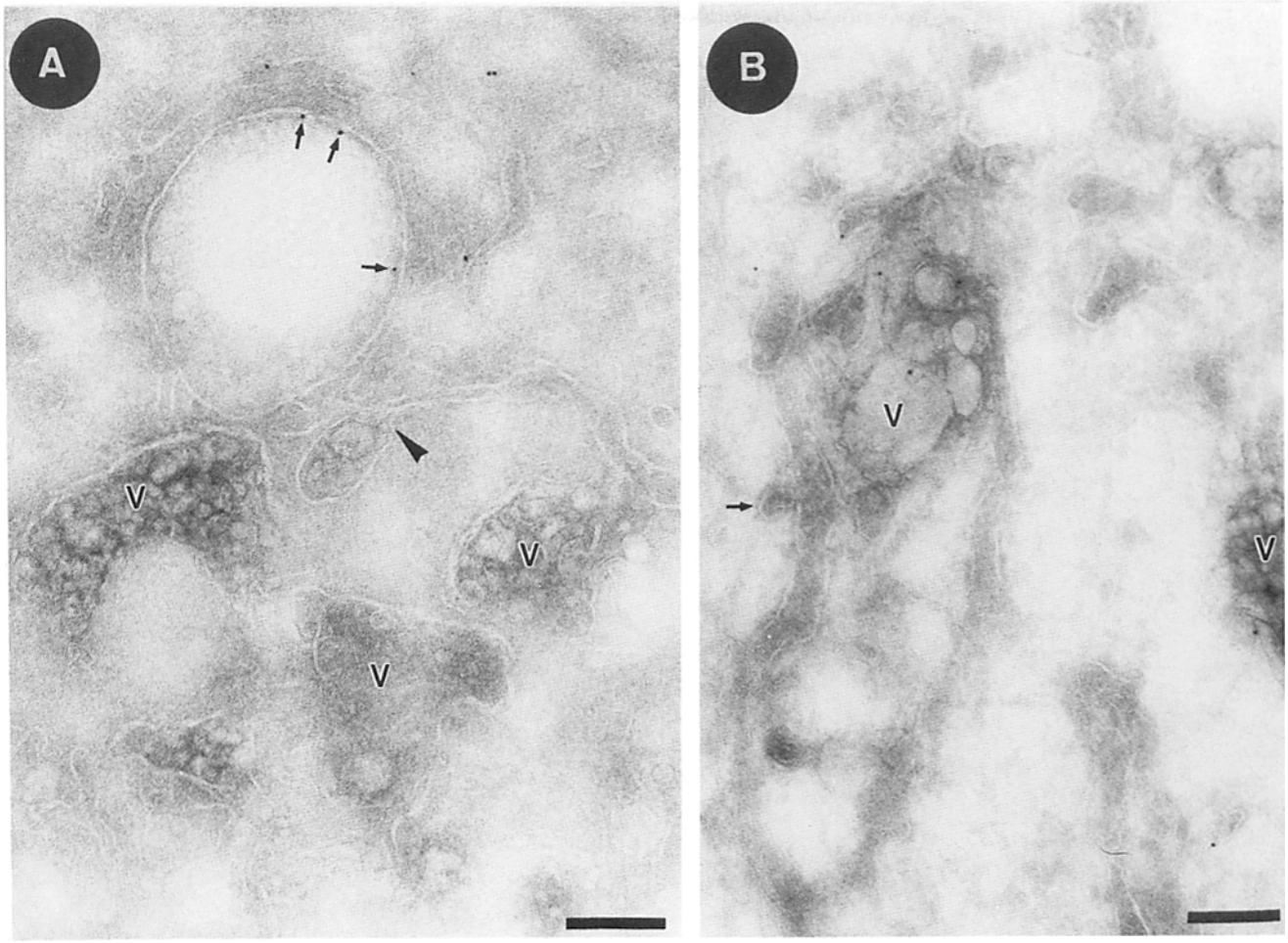

Figure 9. Structures of endosomes in cryosections (2-min internalization of HRP) labeled with anti-HRP and protein A-gold. In *A* the gold is predominantly localized to the periphery of the endosome tubulo-reticular parts (*small arrows*). Although the inner membrane is not visualized, by analogy to the other figures in this paper, we consider it likely that it is present. Endosome vesicles (*V*) are evident in *A*, as well as a continuity between one of these vesicles and the tubulo-cisternal parts of the endosome (*arrowhead*). In *B* the complex nature of endosome structures is evident with vesicular parts (*V*) in continuity with tubulo-cisternal parts. The arrow indicates a possible budding profile which appears to have a cytoplasmic coat associated with it. Bars, 200 nm.

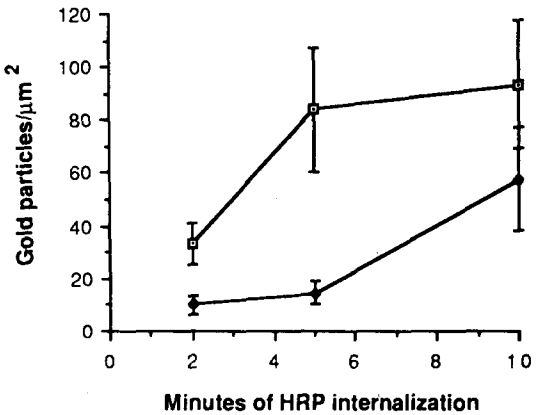

Figure 10. Quantitation of HRP immunogold labeling over early endosomes after internalization of 10 mg/ml HRP by the cells for 2, 5, or 10 min at 37°C before fixation. The open squares show the results for the tubulo-cisternal structures while the solid squares indicate the vesicular structures. Cryosections were labeled with anti-HRP and protein A-gold.

plasma membrane we estimated that coated pits occupy 1.6 ± 0.3% of the plasma membrane surface (in agreement with Anderson et al., 1977). Assuming these pits will give rise to coated vesicles of 100 nm diam, this amount of surface would give rise to 1,170 coated vesicles. From the biochemical measurements of fluid-phase uptake we estimated that 850–1,130 coated vesicles should leave the cell surface each minute. Together, these data indicate that the lifetime of a cell surface coated pit is ~1 min.

Total Surface Area of Membranes in BHK Cells

Surface Area of the Inner and Outer Mitochondrial Membranes. Since we had previously measured the absolute volumes and surface areas of the endoplasmic reticulum, Golgi complex, and the plasma membrane (Griffiths et al., 1984*a*, 1989) and here present estimates for the endocytic pathway, we also determined the total volume and surface areas of the one remaining large pool of membranes in the cell, the mitochondria. Taking the mean cell volume to be

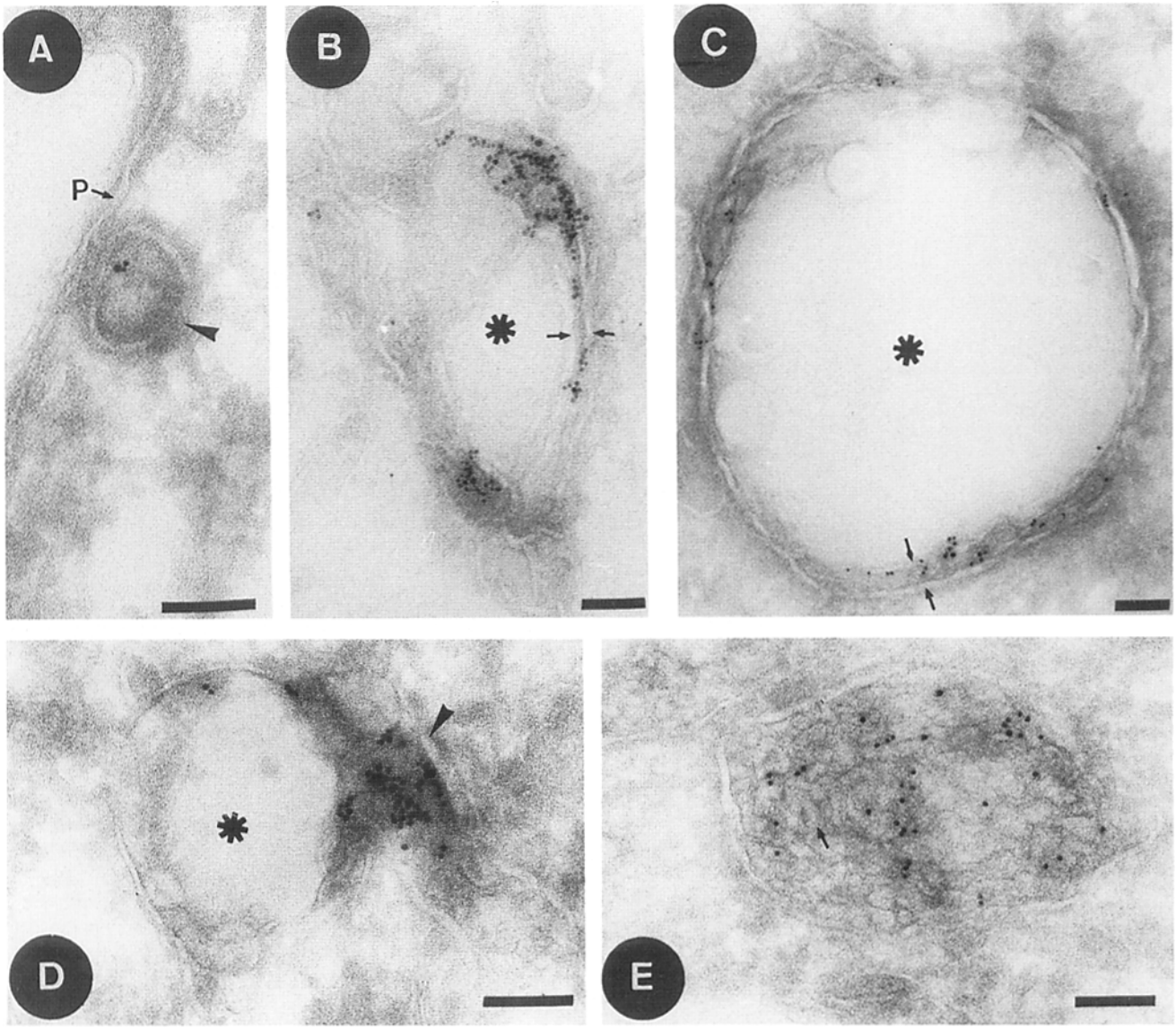

Figure 11. Structure of endosomes in cryosections of cells that had internalized BSA–gold for 10 min at 37°C. *A* shows a labeled clathrin coated vesicle (*arrowhead*) adjacent to the plasma membrane (*P*). *B* and *C* show typical endosome tubulo-cisternal structures: the arrows indicate the two closely apposed membranes. In *D* a larger vesicular structure is seen (*arrowhead*) in continuity with the cup-shaped structure. Note the amorphous appearance of the "space" enclosed by the cup-shaped structures (*asterisks*) in *B–D*. *E* shows a labeled endosome vesicle. The tubular nature of the membrane structures in the lumen is evident (*arrow*). Bars, 100 nm.

1,400 μm^3 (Griffiths et al., 1989) and without taking into account any correction factors (see Paumgärtner and Weibel, 1978) the absolute volume occupied by the mitochondria was estimated to be ~67 μm^3 per cell; the surface areas of the outer and inner membranes were 1,080 and 3,590 μm^2, respectively. Table IV lists the surface areas and volumes of the major membrane compartments of the BHK cell. The value of 15,860 μm^2 for the total membrane surface must be considered an underestimate since it does not include transport vesicles, the TGN, other unidentified membrane compartments, or the membranes contained within endocytic structures.

Discussion

The aim of this study was to measure the volume and surface areas of the organelles that make up the endocytic pathway in BHK cells. A schematic diagram of these organelles is shown in Fig. 12. The stereological estimates of the organelles, visualized by their progressive filling with horseradish peroxidase, comprised the major part of the study. The data indicate that the volume density of HRP-labeled compartments increased rapidly in the first 2 min after addition of the marker and then remained constant for the next 13–18 min. This period was followed by a second rapid increase in volume, between about 20 and 30 min. With respect to the plateau (between 2 and 15–20 min) our interpretation is as follows. Within 2 min HRP is delivered to all endosome structures and the HRP-DAB reaction product completely fills the lumen of these organelles. With increasing time, more HRP solution enters the endosomes, but the volume remains constant, presumably due to an efflux of fluid

Table IV. Summary of Membrane Surface Areas and Volumes of BHK Organelles

	Absolute surface	Absolute volume
	μm^2	μm^3
Cell*		1,400 ± 220
Cytoplasm*		1,050 ± 210
Plasma membrane*	2,200 ± 470	
Coated pits	35 ± 6‡	
ER* (including nuclear envelope)	5,870 ± 990	101 ± 18
Golgi stack	1,960 ± 540	20 ± 5
Endosomes§	430 ± 105	7 ± 2
Lysosomes and prelysosomes	370 ± 113	37 ± 11
Mitochondria		
Outer membrane	1,080 ± 280	
Inner membrane	3,950 ± 711	
Total membrane	15,860 ± 3,209	

* These values are obtained from Griffiths et al., 1989.
‡ This value is included in the plasma membrane total.
§ Organelles that react with HRP up until the 15-min time point.

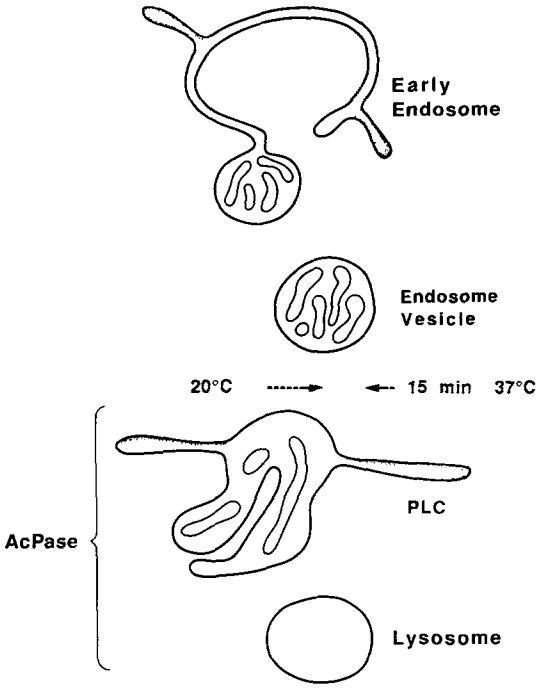

Figure 12. Schematic diagram of the main compartments of the endocytic pathway as described in this paper. The 15-min time point at 37°C and the 20°C block is indicated after the proposed budding-off of the endosome vesicle and before the prelysosome compartment (*PLC*). Note, in addition, that detectable amounts of HRP appear to 'leak' through the 20°C block into the first AcPase compartment—the PLC. The latter is considered to be equivalent to the cation-independent MPR-enriched compartment (Griffiths et al., 1988). We have no direct evidence for this compartment in BHK cells since our anti-MPR antibodies do not react with these cells at the EM level: for reasons given in the discussion, however, we believe it is likely that AcPase does react with two functionally distinct late endocytic structures, as indicated.

back to the medium (Besterman et al., 1981; Adams et al., 1982; Thilo, 1985; Swanson et al., 1985). As the cell-associated HRP activity continues to increase at these early times, the concentration of HRP in the endosomes must increase. This increase was demonstrated directly by quantitating HRP on cryosections. We assume that some HRP moves to later compartments during this period, but in amounts below the level of detection. After 15–20 min a second rapid increase in volume density corresponds to the delivery of significant amounts of HRP to the later stages of the endocytic pathway, the prelysosomes and lysosomes. This interpretation is similar to that given by Steinman et al. (1976) who described the first plateau of volume density (which occurred after 5 min in their study) as filling of the "pinosome" compartment and the second plateau as filling of the "secondary lysosome" compartment, by which they referred to all structures distal to the pinosomes.

The volume and surface densities of the HRP-labeled compartments in BHK cells can be compared to those reported by Steinman et al. (1976) for L cells and macrophages. The endosome and lysosome volumes of BHK and L cells are very similar, though the membrane areas of L cell endosomes and lysosomes (expressed as a proportion of the cell surface area) are significantly smaller than in BHK cells. In contrast, the volume of the secondary lysosome compartment in macrophages is very similar to the AcPase-containing compartment of BHK cells, while the surface areas of BHK cell endosomes and lysosomes are similar to those of the corresponding compartments in macrophages. Significantly, however, the pinosome volume in macrophages is five times larger than the endosomes in BHK cells. The reasons for these differences are unclear. Variations between cell types will undoubtedly provide some explanation; however, the observation that HRP can stimulate the rate of fluid-phase endocytosis in macrophages (Swanson et al., 1985), but has no such effect in BHK cells, suggests that the systems are not directly comparable. In addition, the significant differences that we observe in the morphology of the organelles, especially endosomes, will certainly affect the measurement of the compartment's dimensions. Endosomes, defined here as those structures that label with HRP between 2- and 15-min internalization, are clearly complex in three dimensions. Previous published work has indicated that these organelles contain tubular, cisternal, and vesicular components (see, for example, Wall et al., 1980; Geuze et al., 1983; Hopkins, 1983). Our experiments here show that the total surface area of the endosomes, as well as the volume of the tubulo-cisternal parts of the early endosome, was significantly greater than that of the vesicular parts (Table III) and argues against the notion that the bulk of the volume of the endosome is in the vesicular structures. The cisternal parts of the endosome, which presumably contains the bulk of the volume, are extensive and show a striking tendency to form curved, bowl-shaped organelles enclosing an ill-defined space. This has also been confirmed by serial sectioning (results not shown). The fact that we observe similar structures by three different preparation regimes, namely conventional plastic sections, freeze-substituted specimens, and cryosectioning, makes it unlikely that these structures are artifacts. The cisternal structures are, however, obviously labile and often show a tendency to "explode" so that the HRP–DAB reaction product leaks into the enclosed space. In retrospect, we believe that some of the structures referred to in the previous studies (Steinman et al., 1976; Marsh et al.,

1986; de Chastellier et al., 1987) as "vesicles" may, in fact, have been poorly preserved bowl-shaped cisternae. Furthermore, these structures are not unique to BHK cells and have been observed in many different cell types including L cells and macrophages (Griffiths, G., unpublished data). The nature of the space enclosed by the cisternae is unclear. In plastic sections it is often filled by myelin-like arrays which we believe to be a preparation artifact since these structures were not seen in routine cryosections of aldehyde-fixed cells, nor in hydrated cryosections (sections of rapidly cooled, unfixed cells viewed in the vitreous state in the cold stage of the electron microscope [McDowall et al., 1989]). The space often appears to be in continuity with, but more electron transparent than, the surrounding cytosol and in fixed cryosections it is always completely electron transparent.

In addition to the tubulo-cisternal parts of the endosome, vesicular structures were also observed. We have referred to all structures larger than 80 nm in cross section that label with HRP in the first plateau as vesicles. Many but not all of these structures are clearly continuous with the tubulocisternal elements; all are characterized by the presence of internal tubular membranes, the significance of which is unclear. In contrast to the proposed artifactual myelin-like arrays in the spaces enclosed by the endosomal cisternae, we believe these internal membranes to be real structures. They are evident in our cryosections of fixed cells and also to some extent in unfixed, hydrated cryosections (McDowall et al., 1989). We have noted similar structures in two other studies. In NRK cells 300–400-nm vesicles are labeled when various gold-conjugated endocytic markers are internalized at 20°C, and they appear to be proximal to the MPR-containing prelysosomal compartment (Griffiths et al., 1988). Secondly, in nocodazole-treated BHK cells, very similar vesicles accumulate VSV-G protein which has been implanted into the plasma membrane by low pH fusion (Gruenberg et al., 1989). The latter study demonstrated that these vesicles are structurally and functionally distinct from the tubulocisternal endosomes and, furthermore, suggested that they require functional microtubules for transport to a later stage of the endocytic pathway. The kinetic data of Gruenberg et al. (1989) and Schmid et al. (1988) predicts that, after 15-min internalization, HRP will have gained access to two functionally distinct endosome compartments. Thus, the endosome vesicles may be involved in transport to the prelysosome/lysosome compartments and thus may also, at least in part, be the morphological counterpart of the "late endosomes" in the study of Schmid et al. (1988). Our volume density measurements, however, do not allow us to distinguish between these two compartments. It should also be noted that we made no attempt in our stereological analysis to distinguish between free vesicles and those in continuity with the tubular-cisternal parts of the endosomes.

The second increase in volume seen after 20 min of HRP internalization was interpreted by Steinman et al. (1976) to represent the filling of the secondary lysosome compartment. We would argue that in BHK cells the compartment labeled at times later than 20 min corresponds to at least two distinct compartments, prelysosomes and lysosomes, that are both AcPase-positive. It is now becoming clear that this traditional marker for lysosomes is also present in at least two compartments that can be distinguished from lysosomes. The first of these compartments is the TGN (Novikoff and Novikoff, 1977; Hand and Oliver, 1984) which is primarily a component of the biosynthetic exocytic pathway rather than of the endocytic pathway (Griffiths and Simons, 1986). Second, in NRK cells, chicken erythroblasts, and Madin–Darby canine kidney cells, the prelysosomal compartment also reacts significantly for AcPase. This prelysosomal compartment is distinguished from lysosomes by the presence of high concentrations of MPR and by the fact that it labels with endocytic markers at earlier times than do the lysosomes (Griffiths et al., 1988; Griffiths, G., R. Matteoni, R. Back, and B. Hoflack, submitted for publication; Parton et al., 1989). The cytochemical demonstration of AcPase activity as well as the immunocytochemical evidence for other lysosomal enzymes (Griffiths et al., 1988) is consistent with the notion that the prelysosomal compartment is the delivery site for newly synthesized lysosomal enzymes targeted from the TGN. Since our antibodies against MPR do not react with BHK cells we were unable to make the distinction between the prelysosomes and lysosomes in this study. Nevertheless, the similarity in structure between many of the AcPase-reactive structures in the BHK cell and the MPR-enriched, AcPase-positive compartment in NRK cells strongly suggests that AcPase marks both lysosomes and prelysosomes in BHK cells.

After 2 h at 37°C the HRP-labeled structures represent 1.5% of the cytoplasmic volume. The total volume density of AcPase-reactive vesicular structures, excluding the TGN, was 3.5%. Although this value may be an underestimate (for reasons given in Results) it is, nevertheless, at least twice the volume of HRP-labeled structures after 2-h labeling at 37°C. This suggests that a significant fraction of the total lysosome (or prelysosome) population did not receive HRP during this time. After 2-h labeling and a 2-h chase, however, the volume of the labeled structures increased to ~3.8%, which suggests that the entire lysosome compartment is accessible to HRP, but only after relatively long periods of endocytosis.

The mechanism(s) by which ligands and content are transported from endosomes to lysosomes is not understood. Helenius et al. (1983) put forward two models. The first, the maturation model, proposes that early endosomes continually form by fusion of incoming endocytic vesicles and mature into lysosomes by processes that involve acidification, relocation of the organelles from the periphery to the perinuclear region, selective removal of nonlysosomal components from the maturing organelles, and simultaneous inclusion of lysosome components. The alternative theory is that endosomes exist as one or more stable compartments through which endocytosed membrane and ligands pass, and that transport to and from these preexisting endosomes occurs by vesicular transport. The experiments described here, together with much of the existing data, do not allow an unequivocal distinction to be made. However, we believe that our data are more consistent with the idea that incoming vesicles fuse with, and deliver their contents to, organelles of a preexisting early endosome compartment (see also de Chastellier et al., 1987). In the alternative maturation model, in which coated vesicles would fuse together to assemble endosomes, it is hard to envisage how endosomes could maintain a constant volume and surface area between 2 and 15 min after the addition of HRP while allowing for a constant influx of fluid and, at the same time, for a concentration of the marker within endosomes. A further argument in support of a preexisting early endosome compartment is the three-dimensional complexity of these organelles that is evident in this study.

Our data enable us to estimate the total surface area of

membrane in BHK cells to be 15,860 μm^2. (We emphasize that, since we have ignored the pool of internal intravesicular membranes present within endosomes and prelysosomes, this must be taken as a minimum estimate.) During log phase growth BHK cells must synthesize at least this amount of membrane each generation (~16 h), or 16.5 μm^2/min (11.3 μm^2 if we ignore the mitochondria). Most of the lipid and protein components of this membrane are synthesized in the ER. As the ER itself accounts for 54% of the cellular membrane surface (excluding mitochondria), this fraction of the newly synthesized membrane is presumably retained in the ER. Thus, a minimum net surface area equivalent to ~5 μm^2 (~0.1% of the ER surface area) of newly synthesized membrane must be exported out of the ER each minute. Presumably this membrane will be required for the growth of the Golgi complex, the plasma membrane and endocytic organelles which must also double every generation. Since the Golgi complex accounts for 18% of the total surface area (excluding mitochondria) we would expect that, of the membrane that leaves the ER, this percentage would be retained by the Golgi (~2 μm^2). This would leave an estimated 3.2 μm^2/min of newly synthesized membrane to exit from the TGN. We recently estimated that in BHK cells the area of membrane exported from the TGN to the plasma membrane is, at most, 2.7 μm^2/cell per minute (Griffiths et al., 1989). This estimate is in reasonable agreement with values obtained for the rate of membrane secretion in the thyroid gland (2–3 μm^2/min; Johanson et al., 1984) and parotid gland (11 μm^2/min; Cope and Williams, 1973). Thus, the net export of newly synthesized membrane from the TGN appears to be in the same order of magnitude as the total amount of membrane that is exported. A striking conclusion, therefore, is that all of the membrane involved in transport from the TGN to the plasma membrane may be accounted for by the export of newly synthesized membrane rather than by recycling from the plasma membrane or endosomes.

In conclusion, our data indicate that the average BHK cell, with a volume of 1,400 μm^3 and a plasma membrane surface area of 2,200 μm^2, internalizes ~0.5 μm^3 of fluid per minute and delivers this into the endosomes, which from available kinetic data we argue comprises both the early endosomes and the later, putative endosome carrier vesicles. These organelles collectively have a total volume of 7 μm^3 and a relatively large peripheral surface area of 430 μm^2. Since each round of coated pits to coated vesicles takes 1 min to form, ~35 μm^2 of surface would be internalized per minute, or about the equivalent of 8% of the surface area of the early endosomes. The reaction product of HRP fills the whole of the early endosome compartment after 2 min of internalization and between 2 and 10 min the concentration of HRP increases in approximately linear fashion while the total volume of the labeled compartment remains constant (and does so for a further 5–10 min). After 15–20 min HRP is detected in structures that react significantly with AcPase, which we consider to represent a mixture of prelysosomes and lysosomes. The total volume of these distal structures is more than twice that of the early endosome compartment (although their peripheral surface areas are similar), and this value stays virtually constant until ~90–120 min after the addition of HRP. Finally, the data indicate that over a period of 4 h, the whole of the AcPase-reactive compartments (total volume, 37 μm^3) become accessible to HRP.

We thank Drs. Steve Fuller, Jean Gruenberg, Paul Luzio, Robert Parton, Kai Simons, Brian Storrie, Joel Swanson, Lutz Thilo, John Tooze, and Graham Warren for helpful discussions and for critically reading the manuscript, which was patiently and diligently typed by Rachel Wainwright. The preparations of cells that had cointernalized horesradish peroxidase (HRP) and BSA gold were made by Dr. Claude Antony. The anti-HRP antiserum was a kind gift of Drs. S. Avrameas and L. Teyrnick, Institut Pasteur, Paris that was obtained with the help of Dr. Daniel Louvard.

Mark Marsh is funded by grants to the Institute of Cancer Research from the Cancer Research Campaign and the Medical Research Council.

Received for publication 28 November 1988 and in revised form 1 August 1989.

References

Adams, C. J., K. M. Maurey, and B. Storrie. 1982. Exocytosis of pinocytic content by Chinese hamster ovary cells. *J. Cell Biol.* 93:632–637.

Anderson, R. G. W., M. S. Brown, and J. L. Goldstein. 1977. Role of the coated endocytic vesicle in the uptake of receptor bound low density lipoprotein in human fibroblasts. *Cell.* 10:351–364.

Bergeron, J. J. M., J. Cruz, M. N. Khan, and B. I. Posner. 1985. Uptake of insulin and other ligands into receptor-rich endocytic components of target cells: the endosomal apparatus. *Annu. Rev. Physiol.* 47:383–403.

Besterman, J. M., J. A. Airhart, R. C. Woodworth, and R. B. Low. 1981. Exocytosis of pinocytosed fluid in cultured cells: kinetic evidence for rapid turnover and compartmentation. *J. Cell Biol.* 99:716–727.

Cope, G. H., and M. A. Williams. 1973. Quantitative analysis of the constituent membrane of paroted acinar cells after induced exocytosis. *Z. Zellforsch. Mikros. Anat.* 8:311–330.

Cruz-Orive, L. M. 1982. The use of quadrate and test-systems in stereology, including magnification corrections. *J. Microsc. (Oxf.).* 125:89–102.

Davoust, J., J. Gruenberg, and K. E. Howell. 1987. Two threshold values of low pH block endocytosis at different stages. *EMBO (Eur. Mol. Biol. Organ.) J.*

de Chastellier, C., T. Lang, A. Ryter., and L. Thilo. 1987. Exchange kinetics and composition of endocytic membranes in terms of plasma membrane constituents: a morphometric study in macrophages. *Eur. J. Cell Biol.* 44:112–123.

Geuze, H. J., J. W. Slot, G. J. A. M. Strous, H. F. Lodish, and A. L. Schwartz. 1983. Intracellular site of asialoglycoprotein receptor-ligand uncoupling: double-label immunoelectron microscopy during receptor-mediated endocytosis. *Cell.* 32:277–287.

Goldstein, J. L., M. S. Brown, R. G. W. Anderson, D. W. Russell, and W. J. Schneider. 1985. Receptor mediated endocytosis: concepts emerging from the LDL receptor system. *Annu. Rev. Cell Biol.* 1:1–39.

Green, J., G. Griffiths, D. Louvard, P. Quinn, and G. Warren. 1981. Passage of viral membrane proteins through the Golgi complex. *J. Mol. Biol.* 152:663–698.

Griffiths, G., and K. Simons. 1986. The trans Golgi network: sorting at the exit site of the Golgi complex. *Science (Wash. DC).* 243:438–443.

Griffiths, G., P. Quinn, and G. Warren. 1983. Dissection of the Golgi complex. I. Monesin inhibits the transport of viral membrane proteins from *medial* to *trans* Golgi cisternae in baby hamster kidney cells infected with Semliki Forest virus. *J. Cell Biol.* 96:835–850.

Griffiths, G., G. Warren, P. Quinn, O. Mathieu-Costello, and H. Hoppeler. 1984*a*. Density of newly synthesized plasma membrane proteins in intracellular membranes. I. Stereological studies. *J. Cell Biol.* 98:2133–2141.

Griffiths, G., A. McDowell, R. Back, and J. Dubochet. 1984*b*. On the preparation of cryosections for immunocytochemistry. *J. Ultrastruct. Res.* 89: 65–78.

Griffiths, G., B. Hoflack, K. Simons, I. Mellman, and S. Kornfeld. 1988. The mannose 6-phosphate receptor and the biogenesis of lysosomes. *Cell.* 52:329–341.

Griffiths, G., S. D. Fuller, R. Back, M. Hollinshead, S. Pfeiffer, and K. Simons. 1989. The dynamic nature of the Golgi complex. *J. Cell Biol.* 108:277–297.

Gruenberg, J., and K. Howell. 1986. Reconstitution of vesicle fusions occurring in endocytosis with a cell-free system. *EMBO (Eur. Mol. Biol. Organ.) J.* 5:3091–3101.

Gruenberg, J., and K. Howell. 1987. An internalised membrane protein resides in a fusion-competent endosome for less than five minutes. *Proc. Natl. Acad. Sci. USA.* 84:5758–5762.

Gruenberg, J., G. Griffiths, and K. Howell. 1989. Characterization of the early endosome and putative endocytic carrier vesicles in vivo and with an assay of vesicles fusion in vitro. *J. Cell Biol.* 108:1301–1317.

Hand, A. R., and C. Oliver. 1984. The role of GERL in the secretory process. *In* Cell Biology of the Secretory Process. M. Canlin, editor. Karger Press, Basel. 48–170.

Helenius, A., I. Mellman, D. Wall, and A. Hubbard. 1983. Endosomes. *Trends Biochem. Sci.* 8:245–250.

Hopkins, C. R. 1983. Intracellular routing of transferrin and transferrin recep-

tors in epidermoid carcinoma A431 cells. *Cell.* 35:321–330.
Hopkins, C. R., and I. S. Trowbridge. 1983. Internalization and processing of transferrin and the transferrin receptor in human carcinoma A 431 cells. *J. Cell Biol.* 97:508–521.
Johanson, V., T. Öfverholm, and L. E. Ericson. 1984. Turnover of apical plasma membrane in thyroid follicle cells of normal and tyrosine-treated cells. *Eur. J. Cell Biol.* 35:165–170.
Kielian, M. C., M. Marsh, and A. Helenius. 1986. Kinetics of endosome acidification detected by mutant and wild-type Semliki Forest virus. *EMBO (Eur. Mol. Biol. Organ.) J.* 5:3103–3109.
Marsh, M., and A. Helenius. 1980. Adsorptive endocytosis of Semliki Forest virus. *J. Mol. Biol.* 142:439–454.
Marsh, M., E.-M. Bolzau, and A. Helenius. 1983. Penetration of Semliki Forest virus from acidic prelysosomal vacuoles. *Cell.* 32:931–940.
Marsh, M., G. Griffiths, G. Dean, I. Mellman, and A. Helenius. 1986. Three dimensional structure of endosomes in BHK-21 cells. *Proc. Natl. Acad. Sci. USA.* 83:2899–2903.
Marsh, M., S. Schmid, H. Kern, E. Harms, P. Male, I. Mellman, and A. Helenius. 1987. Rapid analytical and preparative isolation of functional endosomes by free flow electrophoresis. *J. Cell Biol.* 104:875–886.
McDowall, A., J. Gruenberg, K. Römisch, and G. Griffiths. 1989. The structure of organelles of the endocytic pathway in hydrated cryosections of cultured cells. *Eur. J. Cell Biol.* 49:281–294.
Mellman, I., R. Fuchs, and A. Helenius. 1986. Acidification of the endocytic and exocytic pathways. *Annu. Rev. Biochem.* 55:663–700.
Miller, K., J. Beardmore, H. Kanety, J. Schlessinger, and C. R. Hopkins. 1986. Localization of the epidermal growth factor (EGF) receptor within the endosome of EGF-stimulated epidermoid carcinoma (A 431) cells. *J. Cell Biol.* 102:500–509.
Mueller, S. C., and A. Hubbard. 1986. Receptor-mediated endocytosis of asialoglycoproteins by rat hepatocytes: receptor-positive and receptor-negative endosomes. *J. Cell Biol.* 102:932–942.
Murphy, R. M. 1985. Analysis and isolation of endocytic vesicles by flow cytometry and sorting: demonstration of three kinetically distinct compartments involved in fluid phase endocytosis. *Proc. Natl. Acad. Sci. USA.* 82:8523–8526.
Novikoff, A. B., and P. M. Novikoff. 1977. Cytochemical studies on Golgi apparatus and GERL. *Histochem. J.* 9:525–551.
Parton, R. G., K. Prydz, M. Bamsel, K. Simons, and G. Griffiths. 1989. Meeting of the apical and basolateral pathways of the Madin–Darby canine kidney cells in late endosomes. In press.
Paumgärtner, D., and E. R. Weibel. 1978. Integrated stereological and biochemical studies on hepatocyte membranes. II. Correction of section thickness effects on volume and surface density estimates. *J. Cell Biol.* 77:584–597.
Pearse, B. M. F., and M. S. Bretscher. 1981. Membrane recycling by coated vesicles. *Annu. Rev. Biochem.* 50:85–101.
Schmid, S. L., R. Fuchs, P. Male, and I. Mellman. 1988. Two distinct subpopulations of endosomes involved in membrane recycling and transport to the lysosomes. *Cell.* 52:73–83.
Shio, M. A., N. J. Haley, and S. Fowler. 1979. Characterization of lipid-laden aortic cells from cholesterol-fed rabbits. III. Intracellular localization of cholesterol and cholesterol ester. *Lab. Invest.* 41:160–167.
Simons, K., and S. D. Fuller. 1985. Cell surface polarity in epithelia. *Annu. Rev. Cell. Biol.* 1:243–288.
Small, J. W. 1968. Measurement of section thickness. *In* Proceedings of the 4th European Congress on Electron Microscopy. D. S. Bocciaelli, editor. Tipografia Poliglotta Vaticana, Roma. 609–615.
Smith, P. K., R. I. Krohn, G. T. Hermanson, A. K. Mallia, F. H. Gartner, M. D. Provenzano, E. K. Fujimoto, N. M. Goeke, B. J. Olson, and D. C. Klenk. 1985. Measurement of protein using bicinchoninic acid. *Anal. Biochem.* 150:76–85.
Steinman, R. M., S. E. Brodie, and Z. A. Cohn. 1976. Membrane flow during pinocytosis. *J. Cell Biol.* 68:665–687.
Sullivan, P. C., A. L. Ferris, and B. Storrie. 1987. Effects of temperature and energy production inhibitors on horseradish peroxidase transport through endocytic vesicles. *J. Cell. Physiol.* 131:58–63.
Swanson, J. A., B. D. Yirinec, and S. C. Silverstein. 1985. Phorbal esters and horseradish peroxidase stimulate pinocytosis and redirect the flow at pinocytosed fluid in macrophages. *J. Cell Biol.* 100:851–859.
Swanson, J. A., A. Bushnell, and S. C. Silverstein. 1987. Tubular lysosome morphology and distribution within macrophages depend on the integrity of cytoplasmic microtubules. *Proc. Natl. Acad. Sci. USA.* 84:1921–1925.
Thilo, L. 1985. Quantification of endocytosis derived membrane traffic. *Biochem. Biophys. Acta.* 822:243–266.
Wall, D. A., and A. L. Hubbard. 1985. Receptor-mediated endocytosis of asialoglycoproteins by rat liver hepatocytes: biochemical characterization of the endosomal compartments. *J. Cell Biol.* 101:2104–2112.
Wall, D. A., G. Wilson, and A. L. Hubbard. 1980. The galactose-specific recognition system of mammalian liver: the route of ligand internalization in rat hepatocytes. *Cell.* 21:79–93.
Weibel, E. R. 1979. Stereological Methods. 1. Practical methods for biological morphometry. Academic Press, Inc., New York.